

Figure S1. Related to Figure 1.

A. An example of labeled VS neurons by dye backfilling (magenta) from spinal cord in the *Tg(nefma:gal4; uas:GFP)* fishline. Scale bar: 5 μ m

B. Number of labeled VS neurons (mean \pm SEM) by GFP, by dye backfill from the spinal cord, and co-labeled with both on one side of the brain in the larval zebrafish (5-6 dpf). Right, percentage of VS neurons identified by backfill that are also expressing GFP.

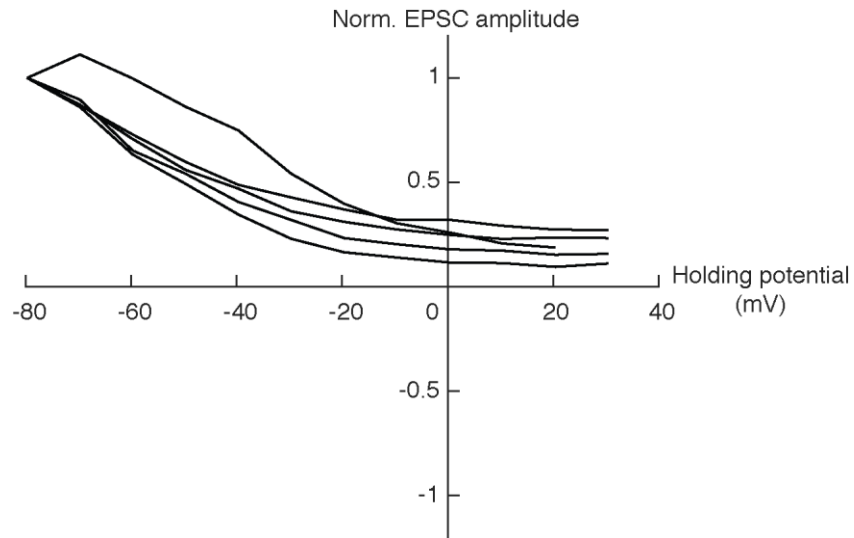


Figure S2. Related to Figure 2.

I-V relationship for the early EPSC component evoked by electrical stimulation on otolith afferents, normalized to EPSC amplitude at -80 mV, $n=5$. Note that early EPSCs do not reverse at 0 mV, consistent with electrical identity. The late EPSC (chemical) component was typically too small to measure at higher holding potential, but in some instances could be seen to reverse [data not shown], consistent with chemical identity.

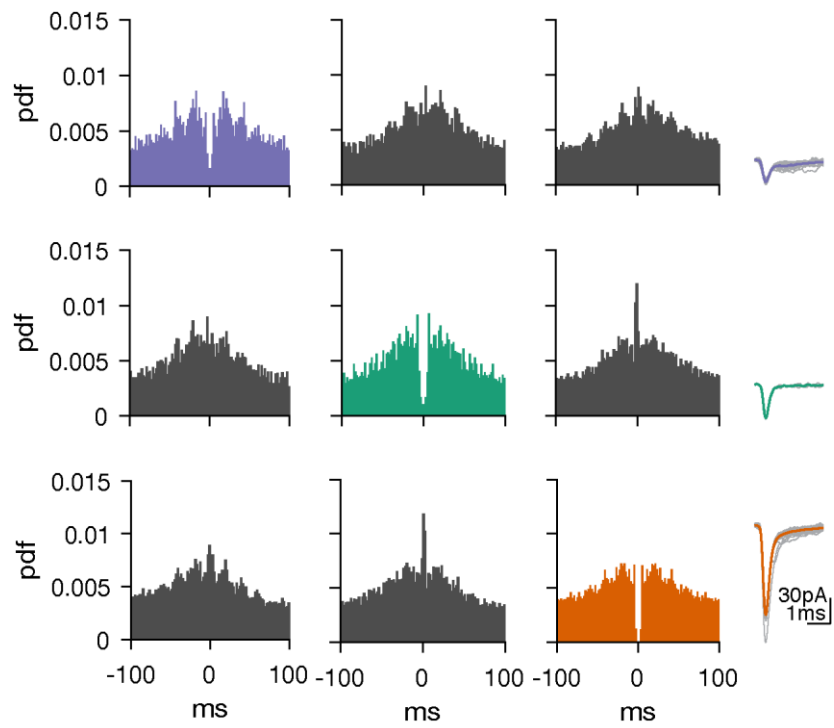


Figure S3. Related to Figure 3.

Auto- and cross-correlograms of three distinct EPSC clusters in one VS neuron. Note that refractory periods only appear in auto-correlograms (colored panels), not in cross-correlograms (gray).

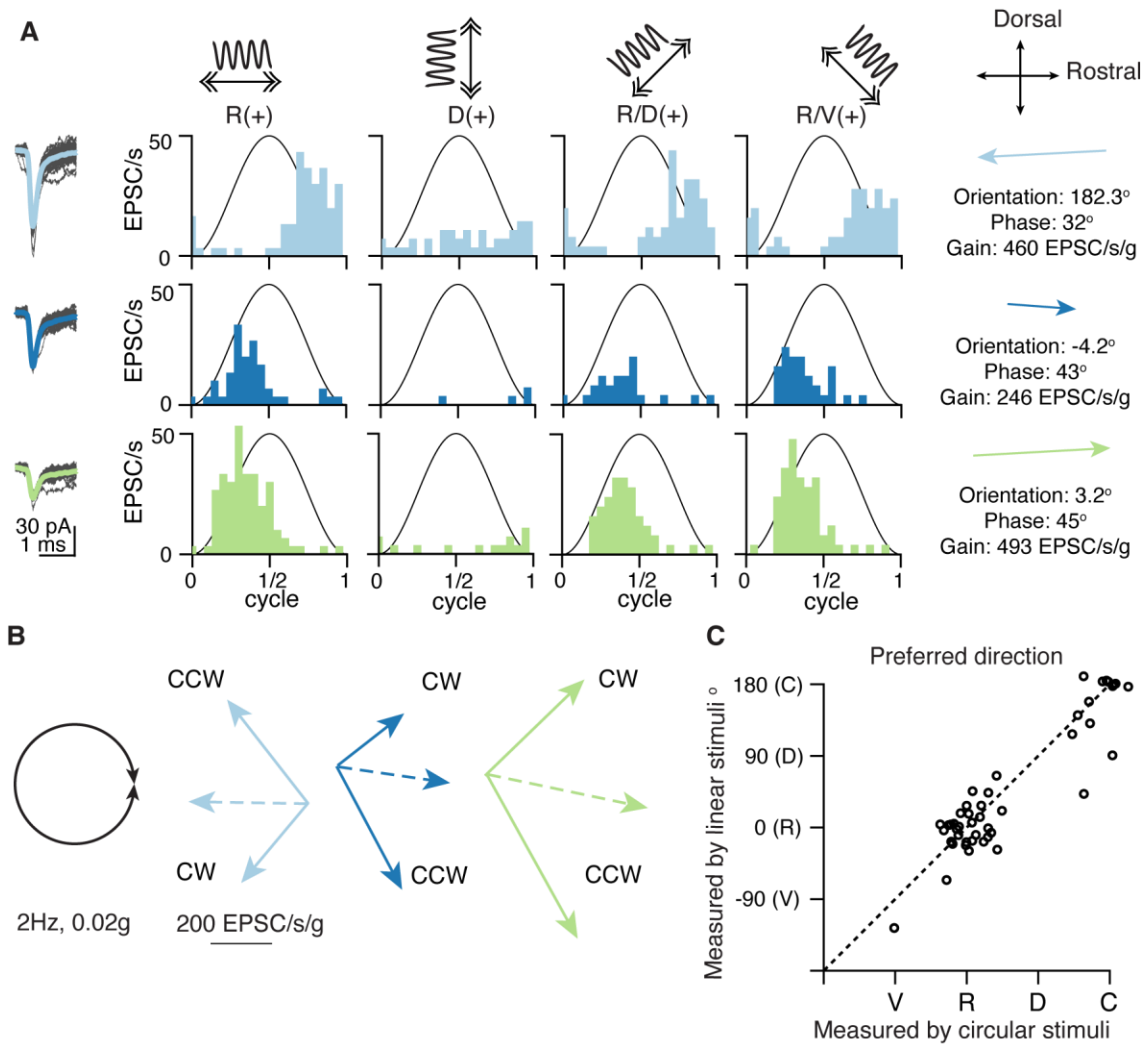


Figure S4. Related to Figure 5.

A. Response vectors of the three afferents converging onto one VS neuron, quantified in the same way as Fig. 5B

B. Response vectors of the same three afferents, measured with clockwise (CW) and counterclockwise (CCW) circular stimuli (left). Solid vectors represent the measured response with CW and CCW stimuli. The dashed vectors represent the vector sums, an estimate of the preferred tuning direction and gain as measured by circular stimuli.

C. Preferred tuning direction measured with 4-axis linear stimuli was highly correlated to preferred tuning direction measured with circular stimuli across the population of inferred otolith afferents ($n=46$). Dashed: unity line; $R=0.92$, $p=5e-20$.

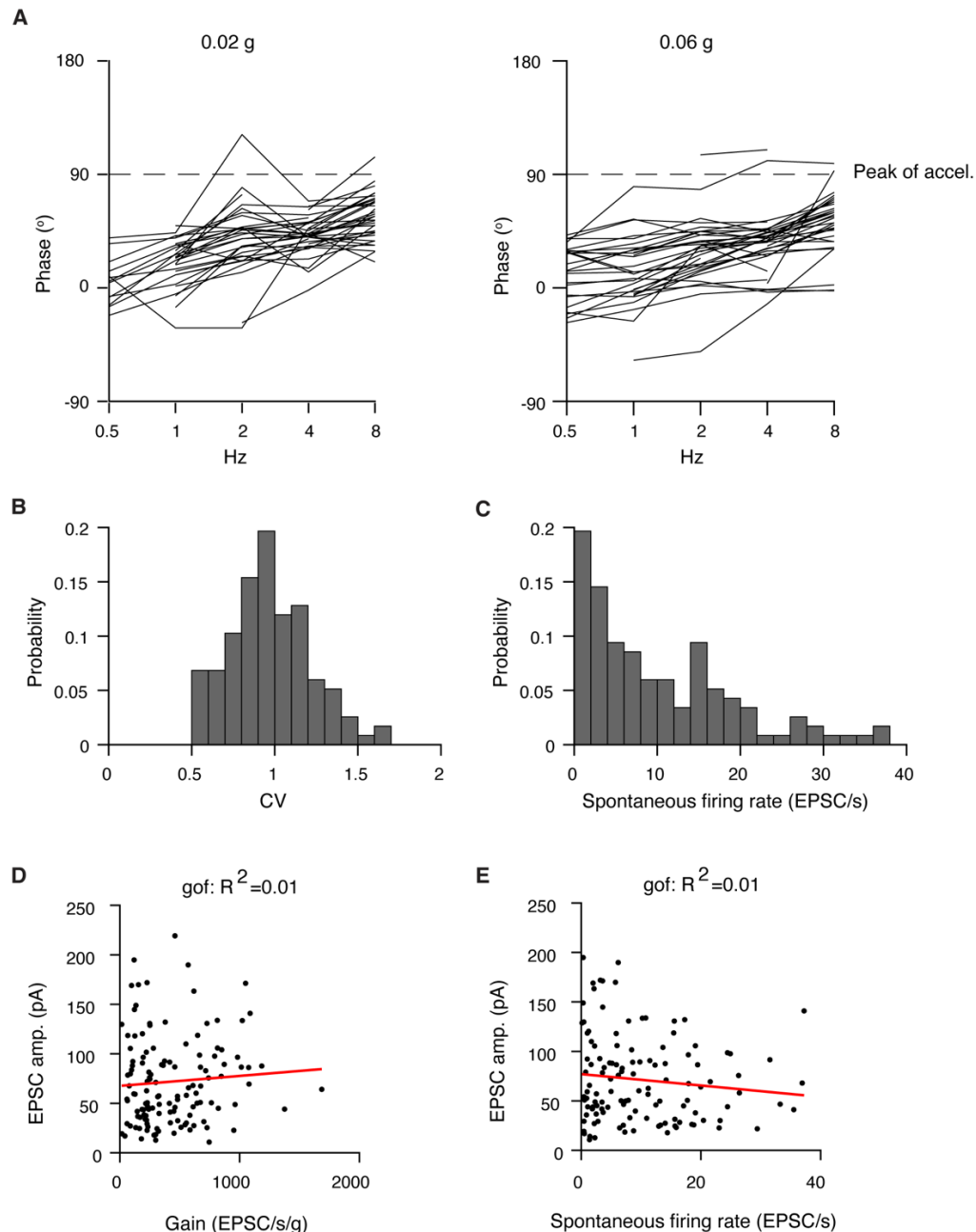


Figure S5. Related to Figure 6.

A. Phase lead relative to peak of acceleration (left, 0.02 g; right, 0.06 g) for all otolith afferents combined. Dashed line indicates peak of acceleration towards preferred direction (either rostral or caudal).

B. Coefficient of variations for spiking of the inferred otolith afferents in the larval zebrafish (n=117).

C. Spontaneous firing rate of inferred otolith afferents in the larval zebrafish. (n=117)

D. No correlation between tuning gain and EPSC amplitudes of inferred afferents (n=129), red: linear fit, gof: goodness of fit.

E. No correlation between spontaneous firing rate and EPSC amplitudes of inferred afferents (n=120), red: linear fit, gof: goodness of fit.

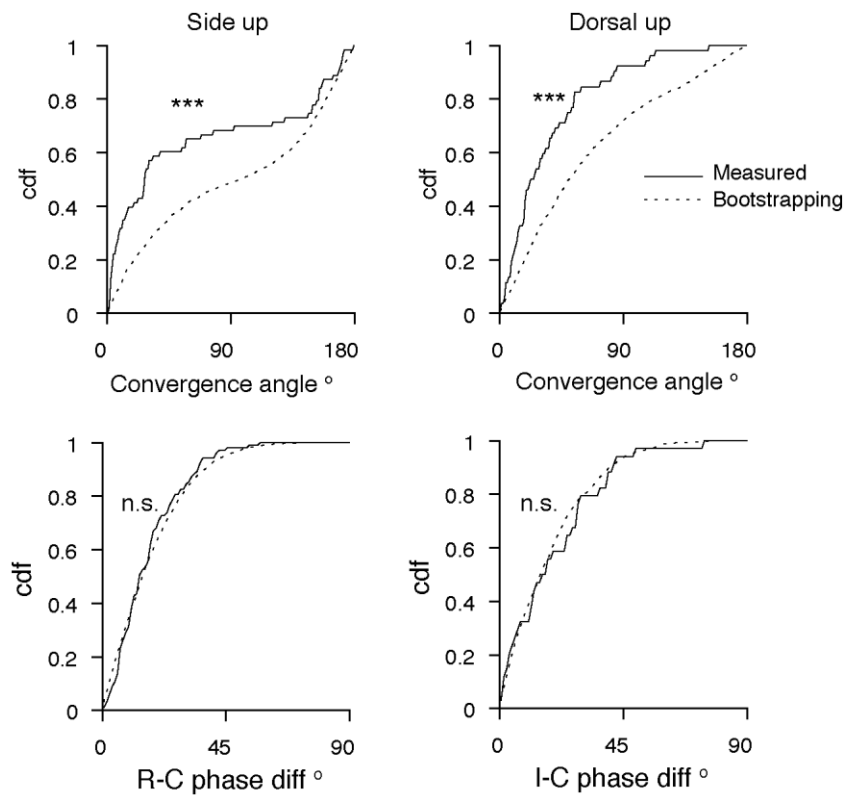


Figure S6. Related to Figure 7.

Cumulative distribution function of convergence angle and phase difference, in measured (solid) and randomly generated (dashed) afferent pairs. Kolmogorov-Smirnov test, $p = 1.3e-5$ (convergence angle, side up), $3.5e-5$ (convergence angle, dorsal up), 0.46 (R-C phase difference), 0.65 (I-C phase difference)

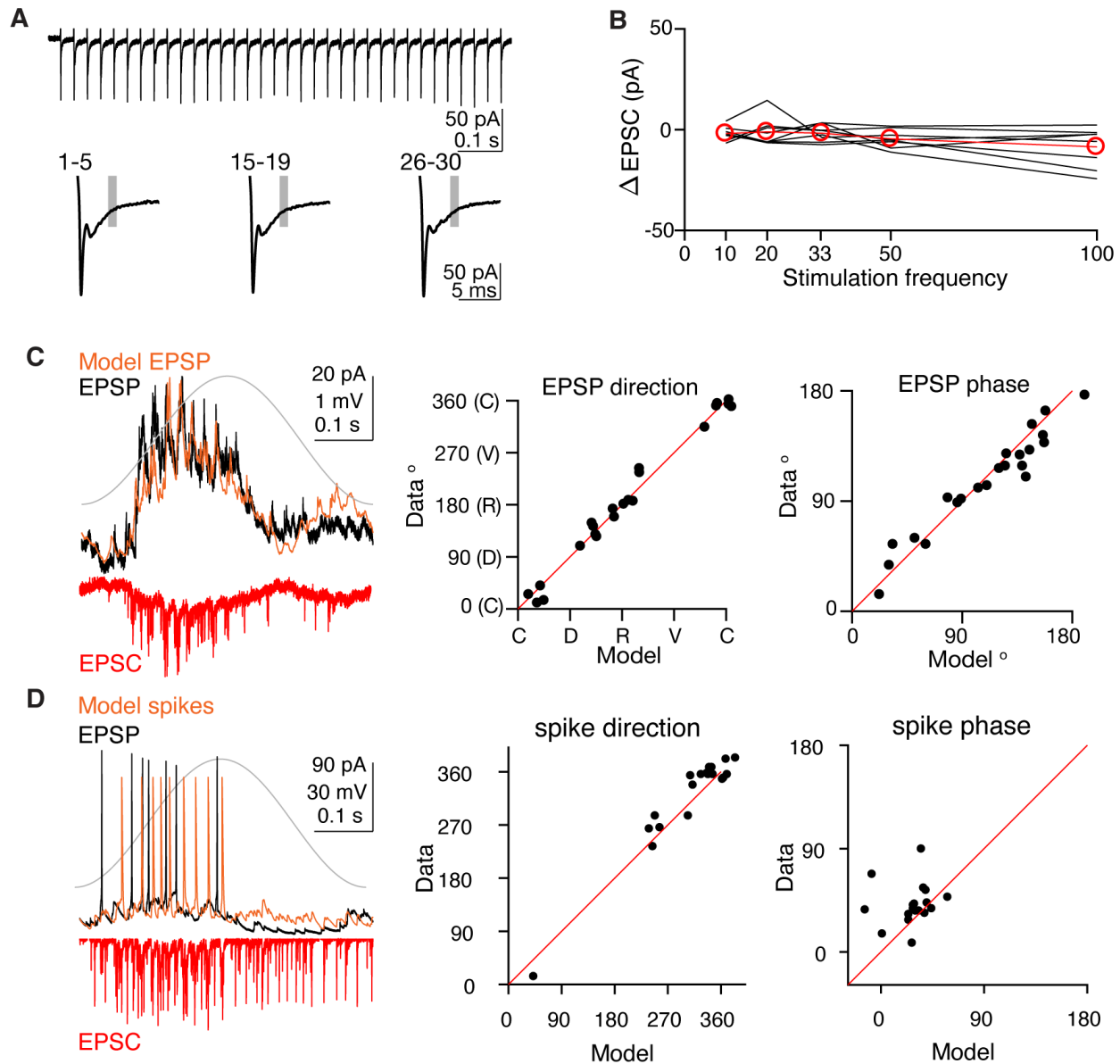


Figure S7. Related to Figure 8.

A. No polysynaptic EPSCs are evoked by electrically stimulating afferents. Top, EPSCs evoked by a train (33 Hz) of electrical pulses on otolith afferents. Bottom, average traces of EPSCs at the beginning (1-5), middle (15-19) and end (26-30) during the train of electric pulses. Shaded area, 4-5 ms (estimated latency of polysynaptic EPSC) after the onset of the pulse. No additional EPSCs are observed in the shaded area for all three average traces.

B. No polysynaptic EPSCs are evoked regardless of stimulation frequency of otolith afferents ($n=8$). $\Delta EPSC$, difference of the average response in the shaded area (4-5 ms) to the last 5 pulses versus the first 5 pulses.

C. EPSC inputs are sufficient to explain EPSP tuning of VS neurons. Left, comparison of EPSC (red) and EPSP (black) responses recorded sequentially in the same VS neuron, to 2 Hz, 0.02 g translational movement on the R(+)-C (-) axis, as well as the

model-generated EPSP (orange). Middle, tuning direction of model-generated membrane potential is consistent with that of recorded EPSPs in the same neuron. Each dot represents the maximum tuning direction of one VS neuron (n=22). Right, tuning phase of model-generated membrane potential is consistent with recorded EPSPs. Each dot represents the phase of one VS neuron in the maximum direction, (n=22). Direction: $R=0.99$, $p=4.2e-19$; Phase: $R=0.97$, $p=1.3e-13$.

D. EPSC inputs are sufficient to explain spike tuning of the VS neurons (n=19). Data as in panel C, for 19 neurons in which both EPSCs and spiking responses to translation were recorded. The inferred best direction (middle) and phase (right) of spiking were well fit between the model and the actual data. Direction: $R=0.97$, $p=7.7e-12$; Phase: $R=0.14$, $p=0.55$.

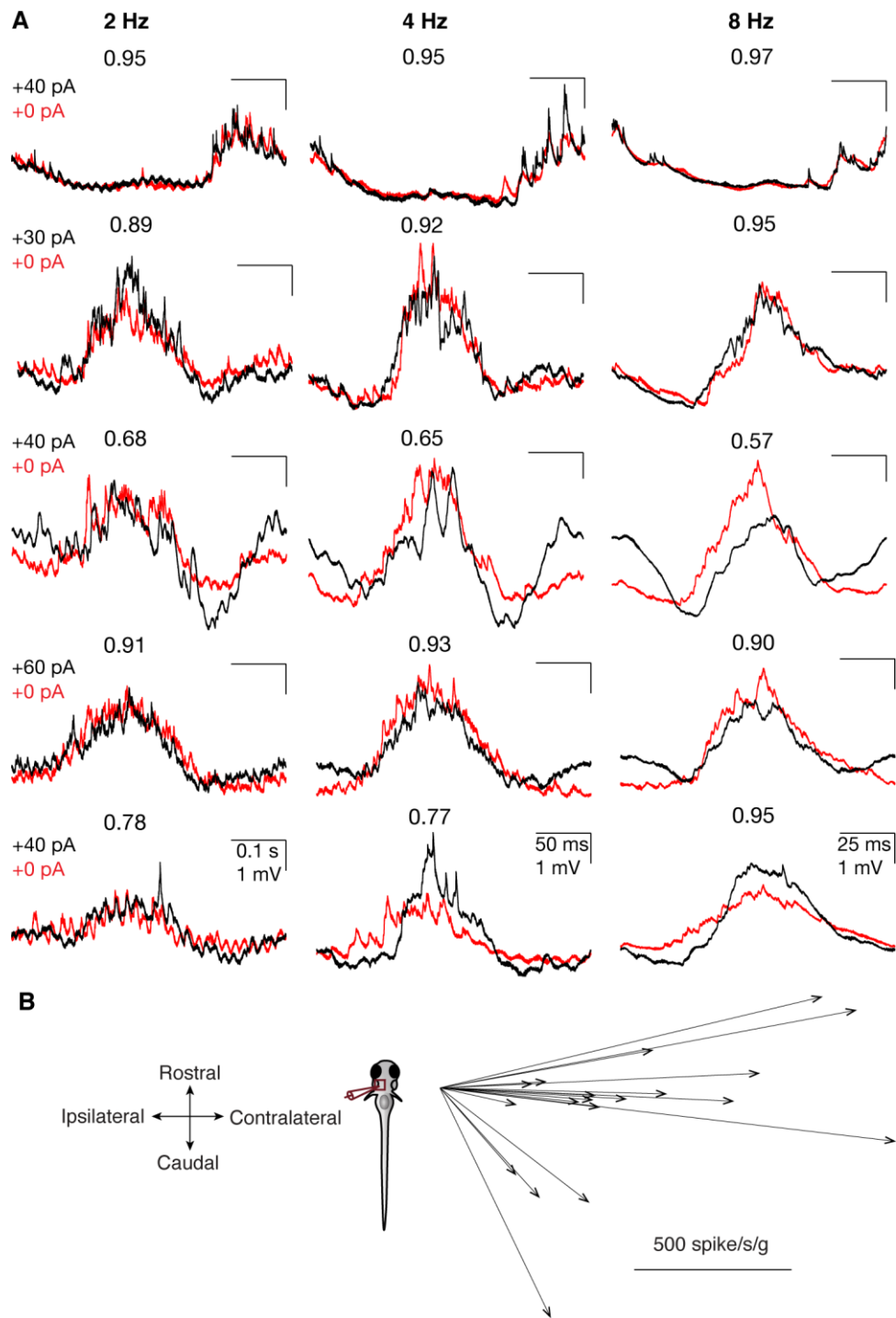


Figure S8. Related to Figure 8.

A. Sensory tuning of 5 different VS neurons (rows) with rheobase current injection (black) and without current injection (red). Responses are shown to three different frequencies of stimulation (columns), with baselines subtracted for easier visual comparison. After spikes were clipped from bias-injected traces, membrane potential was averaged across 10-20 cycles of 0.02 g sinusoidal movements at the given frequencies under each condition. Numbers atop each response are the correlation

coefficient of the two traces and generally indicate highly similar responses between the baseline and current injection conditions.

B. Maximum direction of spiking tuning from VS neurons (n=19) shown in Fig. 8. Fish were oriented dorsal up.